

Advanced synchronization techniques for the Internet of Things

Benoit Geller

► **To cite this version:**

Benoit Geller. Advanced synchronization techniques for the Internet of Things. 2016 International Symposium on Signal, Image, Video and Communications (ISIVC) , Nov 2016, Tunis, Tunisia. pp.180 - 184, 10.1109/ISIVC.2016.7893983 . hal-01624735

HAL Id: hal-01624735

<https://hal-ensta-paris.archives-ouvertes.fr/hal-01624735>

Submitted on 26 Oct 2017

HAL is a multi-disciplinary open access archive for the deposit and dissemination of scientific research documents, whether they are published or not. The documents may come from teaching and research institutions in France or abroad, or from public or private research centers.

L'archive ouverte pluridisciplinaire **HAL**, est destinée au dépôt et à la diffusion de documents scientifiques de niveau recherche, publiés ou non, émanant des établissements d'enseignement et de recherche français ou étrangers, des laboratoires publics ou privés.

ADVANCED SYNCHRONIZATION TECHNIQUES FOR THE INTERNET OF THINGS

Benoit Geller

Department U2IS, ENSTA-ParisTech, Université Paris-Saclay

benoit.geller@ensta-paristech.fr

Invited paper

ABSTRACT

In this paper, we review advanced synchronization techniques for the internet of things. Our study can be directly applied to the single-carrier IEEE 802.15.4 and IEEE 802.15.6 standards. In particular we display the advantages of using a Code-Aided approach and a Bayesian packet-oriented approach. The performances of several phase-locked loop techniques are compared to different Cramer Rao Bounds so that one can see the advantage of respectively the Bayesian approach compared to the on-line approach and of the Code Aided technique compared to the Non Data Aided/ Data Aided approach.

Index Terms—Internet of Things (IoT), Single carrier systems, Phase locked loops (PLL), Code Aided (CA) synchronization, Bayesian synchronization.

1. INTRODUCTION

The Internet of Things (IoT) brings a radical change to the telecommunications paradigm. Up to now, the digital world stopped in our digital terminals and most communications involved human beings. With the IoT, all these frontiers will disappear. Any physical process can be measured with embedded sensors and the IoT aims at creating an “Ambient Intelligence” where many wireless nodes gather and process information to control physical processes. The applications are numerous: industrial surveillance and preventive maintenance (factories 2.0), intelligent buildings, environment control and biodiversity mapping, precision agriculture, health care and medicine, intelligent roads, smart cities, wearables...

Wireless sensors are definitely different from other networks on many points :

- If up to now, a few billions of human beings could communicate, it is expected that in a few years, tens of billions of wireless sensors could be deployed. With the IEEE 802.15.4 standard, the number of connected nodes to an internet gateway can theoretically reach up to 65000 items, which is far more than one is used to manipulate in an ordinary wireless network cell.

- The nodes have generally limited calculus capacities and the targeted prices for the electronic chips are several orders less than the one of traditional chips such as Wifi, and even more 4 or 5G.

- The main problem of a sensor network is its life-time. Often a node is abandoned during its deployment and it has

to rely on its own battery. The main source of energy consumption of a node is due to telecommunications [1] ; for instance, a 2200 mA.h battery node working with a 20mW listening/transmitting consumption will hardly survive more than a couple of weeks ; then the sensor network will have to autonomously insure its self-configurability to bypass the dead relay nodes. Nevertheless, sometimes the sensor network should be able to work reliably during more than 10 years. The only way to reach such a duration is to turn off the radio most of the time with duty cycles inferior to 1%.

In this context, synchronization is of utmost importance. A node should wake up at the right moment to communicate with its environment. In addition, as synchronization is achieved at the front-end before any further processing, it should be reliable enough, not to block any of the following tasks processed by the node. Finally, localization is necessary for more and more applications and localization mainly rely on an accurate synchronization. This is why synchronization has to be accurate even with difficult transmission channels.

There are several kinds of synchronization in each node : packet synchronization, time synchronization, phase synchronization. In this paper, we describe phase synchronization techniques but similar results are available for time synchronization [2]-[6]. In addition, as for simplicity reasons, most presently deployed sensor networks rely on single-carrier technology, we describe several techniques which can improve the traditional phase locked loop (PLL) techniques, in particular in difficult channels (low signal-to-noise ratio, fast fading,...)

This paper is organized as follows. Traditional phase synchronization is reviewed in the next section. In section 3 we describe the advantage of using a code-aided synchronization. Section 4 describes a very low-complexity block Bayesian synchronization technique. Results are compared to Cramer-Rao bounds. Finally a conclusion is drawn at the end of this paper.

2. WELL-KNOWN SYNCHRONIZATION PHASE LOOP TECHNIQUES

We assume that a received modulated signal suffering from AWGN noise (with variance σ_n^2) and from an unknown phase offset θ is sampled at time k , respecting the Nyquist criterion :

$$y_k = a_k e^{jq_k} + n_k, \quad (1)$$

where a_k belongs to a constellation set A . The observation vector $\mathbf{y} = [y_1 \dots y_K]$ stacks K observations and the constellation vector $\mathbf{a} = [a_1 \dots a_K]$ is first assumed to be known (Data Aided –DA approach). The likelihood can be written as :

$$\begin{aligned} p(\mathbf{y}|\theta) &= \prod_{k=1}^K p(y_k|\theta) = \left(\frac{1}{\pi\sigma_n^2}\right)^K e^{-\sum_{k=1}^K \frac{|y_k - a_k e^{j\theta}|^2}{\sigma_n^2}} \\ &= \left(\frac{1}{\pi\sigma_n^2}\right)^K e^{-\frac{\sum_{k=1}^K (|y_k|^2 + |a_k e^{j\theta}|^2 - 2\operatorname{Re}\{y_k \overline{a_k e^{j\theta}}\})}{\sigma_n^2}}. \end{aligned} \quad (2)$$

The Maximum-Likelihood (ML) estimator is a practical popular estimator because if an efficient estimator exists the maximum likelihood procedure will produce it [7]; with model (1), the maximization of the log-likelihood gives:

$$\begin{aligned} \underset{\theta}{\operatorname{ArgMax}}(\ln(p(\mathbf{y}|\theta))) &= \underset{\theta}{\operatorname{ArgMax}}\left(\frac{2}{\sigma_n^2} \sum_{k=1}^K \operatorname{Re}\{y_k \overline{a_k e^{-j\theta}}\}\right) \\ \frac{\partial \ln(p(\mathbf{y}|\theta))}{\partial \theta} &= 0 \Leftrightarrow \\ \frac{2}{\sigma_n^2} \operatorname{Im}\left\{\sum_{k=1}^K y_k \overline{a_k e^{-j\theta}}\right\} &= \frac{2}{\sigma_n^2} \operatorname{Im}\{\mathbf{y} \cdot \mathbf{a} e^{-j\theta}\} \quad (3) \\ &= \frac{2}{\sigma_n^2} \operatorname{Im}\{\mathbf{y} \cdot \mathbf{a} e^{j(\operatorname{Arg}(\mathbf{y} \cdot \mathbf{a}) - j\theta)}\} = 0, \end{aligned}$$

so that equation (3) gives the logical estimator $\hat{\theta}^{(ML)} = \operatorname{Arg}(\mathbf{y} \cdot \mathbf{a})$, which is zero when there is no noise. In practice, one does not need to receive the whole observation vector and proceeds sequentially using a stochastic gradient:

$$\begin{aligned} \hat{\theta}_{k+1} &= \hat{\theta}_k + \gamma \frac{\partial}{\partial \theta} \ln(p(y_k|\theta)) \Big|_{\theta=\hat{\theta}_k} \quad \text{with} \quad \ln(p(y_k|\theta)) \propto \operatorname{Re}\{y_k \overline{a_k e^{-j\theta}}\} \\ &\Leftrightarrow \hat{\theta}_{k+1} = \hat{\theta}_k + \gamma \operatorname{Im}\{y_k \overline{a_k e^{-j\hat{\theta}_k}}\}. \quad (4) \end{aligned}$$

However, in telecommunications networks, one often receives unknown information data (Non Data Aided – NDA approach). When the unknown data are assumed to be equally probable and the alphabet constellation is binary $A = \{-1, +1\}$, the likelihood corresponding to model (1) becomes:

$$\begin{aligned} p(\mathbf{y}|\theta, \mathbf{a}) &= \prod_{k=1}^K p(y_k|\theta, a_k) = \prod_{k=1}^K \frac{1}{\pi\sigma_n^2} e^{-\frac{|y_k - a_k e^{j\theta}|^2}{\sigma_n^2}} \quad (5) \\ p(\mathbf{y}|\theta) &= \left(\frac{1}{\pi\sigma_n^2}\right)^K \prod_{k=1}^K e^{-\frac{|y_k|^2 + 1}{\sigma_n^2} + \frac{+2\operatorname{Re}\{y_k e^{-j\theta}\}}{\sigma_n^2}} \frac{1}{2} + \frac{-2\operatorname{Re}\{y_k e^{-j\theta}\}}{\sigma_n^2} \\ &= \left(\frac{1}{2\pi\sigma_n^2}\right)^K \prod_{k=1}^K e^{-\frac{|y_k|^2 + 1}{\sigma_n^2}} \cosh\left(\frac{2\operatorname{Re}\{y_k e^{-j\theta}\}}{\sigma_n^2}\right), \quad (6) \end{aligned}$$

so that the maximization of the log-likelihood produces the following sequential procedure :

$$\hat{\theta}_{k+1} = \hat{\theta}_k + \gamma \operatorname{Im}\{y_k e^{-j\hat{\theta}_k}\} \tanh\left(\frac{2}{\sigma_n^2} \operatorname{Re}\{y_k e^{-j\hat{\theta}_k}\}\right). \quad (7)$$

(7) looks like (4) for binary symbols, where the tanh() weight of the updating term belongs to $]-1, +1[$ and depends on the signal to noise ratio. When the signal to noise ratio is high, (7) becomes equivalent to the decision feedback loop, whereas when the signal to noise is low, (7) is equivalent to the Costas-loop:

$$\hat{\theta}_{k+1} = \hat{\theta}_k + \gamma' \operatorname{Im}\{y_k^2 e^{-j2\hat{\theta}_k}\}. \quad (8)$$

The sequential updating procedures corresponding to equations (4), (7) and (8) are known as digital Phase Locked Loops (PLL). Not only the PLLs are low complexity algorithms, but they also have an inherent adaptativity feature to time-varying estimation due to the sequential estimation. However, the PLLs also suffer from several drawbacks :

- The choice of the step-size might be problematic. If it is chosen too small, the PLL hardly converges and is unable to follow non stationnarities. If it is chosen too large, the asymptotic MSE remains too large. The choice of an adaptative step-size [8]-[10] can prevent those phenomena but is beyond the scope of this paper.

- Noise can make the PLL diverge from a fixed stable point (Cycle slip problem).

- An arbitrary initialization can make a slow PLL converge (Hang up problem).

- The algorithm can get stuck in a local minimum.

To prevent as much as possible, the latest situations the previous PLLs can be improved as seen in the next sections.

3. CODE-AIDED PHASE LOCKED LOOPS

Clearly, the main goal of a receiver is not to only locally solve the problem of synchronization, but rather to recover reliably some useful data. To achieve this reliability and have a near-Shannon performance, the transmitter is helped by the redundancy of a channel coder. If the synchronization is not good, the reliability of the decoded data will be low and this can be highlighted by the soft information at the output of the decoder [11]-[15].

Some ad-hoc methods take advantage of the inherent link between the quality of the synchronization and the decoder's output by maximizing the average power of the soft information [16]-[17]. Other methods such as [18]-[19] have been devised but suffer from their complexity.

In fact, the PLLs introduced in the previous section can easily be modified to benefit from the decoder's soft output with a moderate complexity increase [20]-[22].

We assume that the observation model is still given by equation (1) but that a soft decoder is able to provide some LLR values Λ_k . If the constellation alphabet A is first supposed to be binary, we have :

$$p(a_k = \pm 1) = \frac{2e^{\pm \frac{\Lambda_k}{2}}}{\cosh\left(\frac{\Lambda_k}{2}\right)} \quad (9)$$

Introducing (9) in the likelihood, we then obtain :

$$\begin{aligned} p(\mathbf{y}|\theta, \mathbf{a}) &= \prod_{k=1}^K p(y_k|\theta, a_k) = \prod_{k=1}^K \frac{1}{\pi\sigma_n^2} e^{-\frac{|y_k - a_k e^{j\theta}|^2}{\sigma_n^2}} \\ p(\mathbf{y}|\theta) &= \left(\frac{1}{2\pi\sigma_n^2}\right)^K \prod_{k=1}^K e^{-\frac{|y_k|^2 + 1}{\sigma_n^2}} \left(\frac{2e^{\frac{\Lambda_k}{2}}}{\cosh\left(\frac{\Lambda_k}{2}\right)} e^{-\frac{-2\text{Re}\{y_k e^{-j\theta}\}}{\sigma_n^2}} + \frac{2e^{-\frac{\Lambda_k}{2}}}{\cosh\left(\frac{\Lambda_k}{2}\right)} e^{-\frac{+2\text{Re}\{y_k e^{-j\theta}\}}{\sigma_n^2}} \right) \\ &= \left(\frac{1}{2\pi\sigma_n^2}\right)^K \prod_{k=1}^K \frac{2e^{-\frac{|y_k|^2 + 1}{\sigma_n^2}}}{\cosh\left(\frac{\Lambda_k}{2} + \frac{2\text{Re}\{y_k e^{-j\theta}\}}{\sigma_n^2}\right)} \end{aligned} \quad (10)$$

As in the previous section, we obtain a sequential algorithm by maximizing at each instant, the following quantity:

$$\text{Max}_{\theta}(\ln(p(y_k|\theta))) = \text{Max}_{\theta} \left(\ln \left\{ \cosh \left(\frac{\Lambda_k}{2} + \frac{2}{\sigma_n^2} \text{Re}\{y_k e^{-j\theta}\} \right) \right\} \right) \quad (11)$$

so that the derivation gives :

$$\frac{\partial \ln(p(y_k|\theta))}{\partial \theta} \propto \frac{2}{\sigma_n^2} \text{Im}\{y_k e^{-j\theta}\} \tanh \left(\frac{\Lambda_k}{2} + \frac{2}{\sigma_n^2} \text{Re}\{y_k e^{-j\theta}\} \right) \quad (12)$$

We then obtain the Code-Aided PLL updating :

$$\hat{\theta}_{k+1} = \hat{\theta}_k + \gamma \text{Im}\{y_k e^{-j\hat{\theta}_k}\} \tanh \left(\frac{\Lambda_k}{2} + \frac{2}{\sigma_n^2} \text{Re}\{y_k e^{-j\hat{\theta}_k}\} \right) \quad (13)$$

Equation (13) is very similar to equation (7). The only difference lies in the argument of the tanh() weight. In the case of equation (13), the weight does not only take into account the SNR, but also the reliability given by the decoder's output.

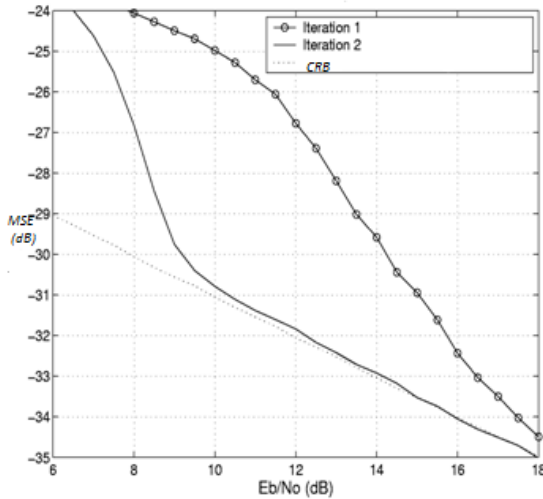


Fig.1. Convergence of the CA synchronizer in 2 iterations

In practice and as illustrated by figure 1, a CA PLL needs (at least) two iterations. When processing the received data at the first iteration, the synchronization device has no information from the decoder's output so that with LLR

values equal to zero, equation (13) is equivalent to equation (7). Then the receiver is able to demodulate its data and provide LLR values which are fed back at the front-end synchronizer working with equation (13). This then gives a more reliable phase estimate vector; it can be seen that sometimes two iterations are sufficient to reach the Cramer-Rao bound [7]. In general, some Exit chart analysis [11] should be made to forecast the convergence conditions but in many situations two or three iterations (between the decoder's output and the PLL's input) are sufficient to obtain a good convergence of the CA phase synchronizer. Clearly with CA synchronization, the synchronizer can take advantage of the decoder soft information as long as the decoder works correctly; this allows some improvement, when compared to NDA mode, from medium to (near Shannon) low SNRs. The previous algorithm described by equation (13) can readily be extended to a QAM constellation alphabet \mathcal{A} of size M . By proceeding analogously, we obtain:

$$\hat{\theta}_{k+1} = \hat{\theta}_k + \gamma \text{Im}\{E_{QAM/y_k}(\bar{a}_k) y_k e^{-j\hat{\theta}_k}\}, \quad (14)$$

where the mean soft symbol is obtained by :

$$E_{QAM/y_k}(\bar{a}_k) = \sum_{a_v \in QAM} \bar{a}_v p(a_v) \quad (15)$$

$$\text{with } p(a_v) = \frac{w(a_v, y_k, \Lambda_k, \hat{\theta}_k)}{\sum_{a_v \in QAM} w(a_v, y_k, \Lambda_k, \hat{\theta}_k)}$$

$$\text{and } w(a_v, y_k, \Lambda_k, \hat{\theta}_k) = e^{-\frac{|y_k - a_v e^{-j\hat{\theta}_k}|^2}{\sigma_n^2} + \frac{M}{2} \frac{B_v \Lambda_k^m}{\sigma_n^2}}$$

Equation (14) is equivalent to equation (4) for the DA case; also, we can simplify equation (14) with a decision directed loop at high SNR. In short, the CA mode allows to achieve a better spectrum efficiency, when compared to the DA mode, and a better performance at lower SNR than the NDA mode.

4. LOW COMPLEXITY BAYESIAN SYNCHRONIZATION

The Bayesian approach is a natural choice when a parameter is time-varying because this feeds some a priori to the estimation process. We add the following Brownian phase model to the observation model (1) :

$$\theta_k = \theta_{k-1} + \xi + w_k, \quad (16)$$

where the phase at time k is modified by a linear drift ξ and some Gaussian noise w_k of variance σ_w^2 . This noise takes into account the poor oscillator's quality as encountered in sensor networks. The phases are stacked in $\boldsymbol{\theta}$. Note that the model described by equations (1) and (16) is neither linear, nor stationary. The MAP approach which weights the likelihood can then take advantage of the natural a priori introduced by equation (16):

$$\begin{aligned} \hat{\boldsymbol{\theta}}^{(\text{MAP})} &= \arg \max_{\boldsymbol{\theta}} p(\boldsymbol{\theta}|\mathbf{y}) \\ &= \arg \max_{\boldsymbol{\theta}} \{p(\mathbf{y}|\boldsymbol{\theta}) p(\boldsymbol{\theta}) / p(\mathbf{y})\} = \arg \max_{\boldsymbol{\theta}} \{p(\mathbf{y}|\boldsymbol{\theta}) p(\boldsymbol{\theta})\} \\ &= \arg \max_{\boldsymbol{\theta}} \{p(\boldsymbol{\theta}, \mathbf{y})\} = \arg \max_{\boldsymbol{\theta}} \{\ln p(\boldsymbol{\theta}, \mathbf{y})\} \end{aligned} \quad (17)$$

Bayesian (resp. Hybrid) Cramer-Rao bounds were created to measure the performance of a random (resp. random and deterministic) parameters [7][23]. These bounds indicate that there is room for a good estimation improvement brought by the Bayesian approach [24]-[27],[34]. Different estimators were devised to approach those bounds but they usually suffer from a complexity brought by the Bayesian canvas[18],[28]-[30]. We now see that the previous PLLs can be easily adapted to the Bayesian context at a very moderate complexity price [31]. We start with a binary constellation set A. With the model given by (1) and (16), the joint probability density can be written as:

$$p(\mathbf{y}, \boldsymbol{\theta}) = p(\mathbf{y} | \boldsymbol{\theta}) p(\boldsymbol{\theta}) \quad (18)$$

$$= p(\theta_1) p(y_1 | \theta_1) \prod_{k=2}^K p(y_k | \theta_k) p(\theta_k | \theta_{k-1})$$

where:

$$p(\theta_k | \theta_{k-1}) = \frac{1}{\sqrt{2\pi}\sigma_w} \exp\left\{-\frac{(\theta_k - \theta_{k-1} - \xi)^2}{2\sigma_w^2}\right\}$$

and $p(y_k | \theta_k) = \left(\frac{1}{2\pi\sigma_n^2}\right)^K e^{-\frac{|y_k|^{+1}}{\sigma_n^2}} \cosh\left(\frac{2\operatorname{Re}\{y_k e^{-j\theta_k}\}}{\sigma_n^2}\right)$ (19)

In order to find the maximum of equation (18), we set

$$\left. \frac{\partial \ln(p(\mathbf{y}, \boldsymbol{\theta}))}{\partial \theta_k} \right|_{\theta_k = \hat{\theta}_k^{(MAP)}} = 0$$

Assuming no initial a priori on θ_1 , we then find:

$$\hat{\theta}_k^{(MAP)} \approx \begin{cases} \theta_2^{(B)} + \frac{2\sigma_w^2}{\sigma_n^2} \tanh\left(\frac{2\operatorname{Re}\{y_2 e^{-j\hat{\theta}_2^{(B)}}\}}{\sigma_n^2}\right) \operatorname{Im}\{y_2 e^{-j\hat{\theta}_2^{(B)}}\} - \hat{\xi} & k=1 \\ \frac{1}{2}(\hat{\theta}_k^{(F)} + \hat{\theta}_k^{(B)}) & 2 \leq k \leq K-1 \\ \hat{\theta}_{K-1}^{(F)} + \frac{2\sigma_w^2}{\sigma_n^2} \tanh\left(\frac{2\operatorname{Re}\{y_{K-1} e^{-j\hat{\theta}_{K-1}^{(F)}}\}}{\sigma_n^2}\right) \operatorname{Im}\{y_{K-1} e^{-j\hat{\theta}_{K-1}^{(F)}}\} + \hat{\xi} & k=K \end{cases} \quad (20)$$

with:

$$\hat{\theta}_k^{(F)} = \hat{\theta}_{k-1}^{(F)} + \frac{\sigma_w^2}{\sigma_n^2} \tanh\left(\frac{2\operatorname{Re}\{y_k e^{-j\hat{\theta}_{k-1}^{(F)}}\}}{\sigma_n^2}\right) \operatorname{Im}\{y_k e^{-j\hat{\theta}_{k-1}^{(F)}}\} \quad (21)$$

and

$$\hat{\theta}_k^{(B)} = \hat{\theta}_{k+1}^{(B)} + \frac{\sigma_w^2}{\sigma_n^2} \tanh\left(\frac{2\operatorname{Re}\{y_k e^{-j\hat{\theta}_{k+1}^{(B)}}\}}{\sigma_n^2}\right) \operatorname{Im}\{y_k e^{-j\hat{\theta}_{k+1}^{(B)}}\} \quad (22)$$

Equation (21) is just like equation (7), whereas equation (22) is similar to equation (21) with the role of the indexes $k+1$ and k being inversed. In other words, the approximate MAP estimator of equation (20) is just the mean of a forward PLL given by equation (21) and of a backward PLL (working from the end of the block towards its beginning). In practice, we can first run an ordinary PLL, then, at the end of the block, we run a backward PLL towards the beginning of the block, we repeat this procedure until convergence (in practice 2 or 3 forward-backward recursions), and in the end, we average at each time index, the last forward and backward estimates to obtain the approximate MAP estimator as described by equation (20). Just like in [32], the initialization has a lower impact because of the various forward and backward iterations, but

differently from [32], the MAP performance improvement is brought by the averaging between the two trajectories.

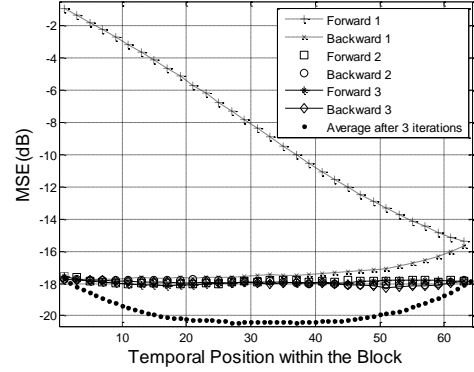


Fig.2. Comparison of the Forward and of the Forward-Backward MAP estimation performance

16QAM ($\sigma_w^2 = 0.0002\text{rad}^2$, $\xi = 0.003\text{rad}$, $N_{S-PLL} = 3$)

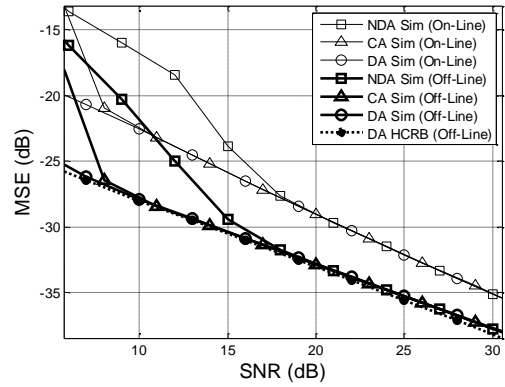


Fig.3 Comparison of the Forward (On-Line) and the Forward-Backward (Off-Line) estimation performance for the NDA/CA/DA modes

The previous algorithm described by equations (20)-(22) can be generalized to any coded QAM systems [33]. Proceeding analogously, we obtain:

$$\hat{\theta}_k^{(MAP)} \approx \begin{cases} \theta_2^{(B)} + \frac{2\sigma_w^2}{\sigma_n^2} \operatorname{Im}\{y_2 E_{QAM}(\bar{a}_2) e^{-j\hat{\theta}_2^{(B)}}\} - \hat{\xi} & k=1 \\ \frac{1}{2}(\hat{\theta}_k^{(F)} + \hat{\theta}_k^{(B)}) & 2 \leq k \leq K-1 \\ \hat{\theta}_{K-1}^{(F)} + \frac{2\sigma_w^2}{\sigma_n^2} \operatorname{Im}\{y_{K-1} E_{QAM}(\bar{a}_{K-1}) e^{-j\hat{\theta}_{K-1}^{(F)}}\} + \hat{\xi} & k=K \end{cases} \quad (23)$$

with :

$$\hat{\theta}_k^{(F)} = \hat{\theta}_{k-1}^{(F)} + \frac{\sigma_w^2}{\sigma_n^2} \operatorname{Im}\{y_{k-1} E_{QAM}(\bar{a}_{k-1}) e^{-j\hat{\theta}_{k-1}^{(F)}}\} \quad (24),$$

$$\hat{\theta}_k^{(B)} = \hat{\theta}_{k+1}^{(B)} + \frac{\sigma_w^2}{\sigma_n^2} \operatorname{Im}\{y_{k+1} E_{QAM}(\bar{a}_{k+1}) e^{-j\hat{\theta}_{k+1}^{(B)}}\}$$

and $E_{QAM}(\bar{a}_k)$ is given by (15). The performance of such an algorithm after $N_{S-PLL}=3$ iterations is displayed in Figure 3 for a (possibly turbo-coded) 16 QAM signal. The advantage of the MAP (Off-line) estimation over the ML (On-line) is very clear with a MSE gain of several dBs for any SNR. In addition, the MAP estimator performance is very near from the HCRB and one recovers that the CA mode stays near the bound for lower SNRs than the NDA mode.

5. CONCLUSION

In this paper, we have presented some single-carrier synchronization algorithms that are able to reach the Cramer-Rao bounds in difficult conditions (phase noise) with a very low complexity. These algorithms are well suited to limited devices as sensor nodes of the IoT. Some future work aims at including the synchronization in a cross-layer context [35]-[36], so as to ease up some localization functionality, often useful with the IoT.

6. REFERENCES

- [1] G. Pottie and W. Kaiser, "Wireless integrated sensor networks", *Communications of the ACM* 43(5) pp. 51-58, 2000.
- [2] I. Nasr, L. Najjar Atallah, S. Cherif, B. Geller, "Time synchronization in IoT Networks: Case of a WBAN", *Proc. of IEEE ISIVC*, Tunis, November 2016.
- [3] I. Nasr, B. Geller, L.N. Atallah, S. Cherif, "Near MAP Dynamical Delay Estimator and Bayesian CRB for QAM Coded Signals", submitted to *IEEE Transactions*.
- [4] I. Nasr, B. Geller, L.N. Atallah, S. Cherif, "Performance Study of a New Near Maximum Likelihood Code-Aided Timing Recovery Technique", *IEEE Transactions on Signal Processing*, vol. 64, pp. 799-811, Feb. 2016.
- [5] I. Nasr, L. Najjar Atallah B. Geller, S. Cherif, "CRB Derivation and New Code-Aided Timing Recovery Technique for QAM Modulated Signals", *Proc. of ICC 2015*, London, June 2015.
- [6] I. Nasr, L. Najjar Atallah, S. Cherif, B. Geller, J. Yang, "A Soft Maximum Likelihood Technique for Time Delay Recovery", *Proceedings of IEEE COMNET*, Tunis, Mars 2014.
- [7] S. Kay, "Fundamentals of statistical signal processing", vol.1, Prentice Hall.
- [8] J.M. Brossier, P.O. Amblard, B. Geller, "Self Adaptive PLL for General QAM Constellations", *Proceedings of EUSIPCO*, pp 631-635 Toulouse, Sept 2002.
- [9] B. Geller, V. Capellano, J.M. Broissier, "Equalizer for High Rate Transmission", *Proceedings of OCEANS'94*, IEEE Oceans engineering Oceans Engineering for Today's Technology and Tomorrow's Preservation, Brest, Sept. 1994.
- [10] B. Geller, V. Capellano, J.M. Brossier, A. Essebbar, G. Jourdain, "Equalizer for Video Rate Transmission in Multipath Underwater Communications", *IEEE Journal of Oceanic Engineering*, vol. 21, no 2, pp 150-156, April 1996.
- [11] S. Lin, D. Costello, "Error Control Coding", 2nd ed., Pearson Prentice Hall, 2004.
- [12] C. Berrou "Codes et turbo codes", Collection Iris, Springer.
- [13] I. Diatta, D. De Geest, B. Geller, "Reed Solomon Turbo Codes for High Data Rate Transmission", *Proceedings of IEEE VTC*, pp. 1023-1027, Milan, May 2004.
- [14] B. Geller, I. Diatta, J.P. Barbot, C. Vanstraceele, F. Rambeau, "Block Turbo Codes : From Architecture to Application", *Proceedings of IEEE ISIT*, Seattle, July 2006.
- [15] C. Vanstraceele, B. Geller, J.P. Barbot, J.M. Brossier, "A Low Complexity Block Turbo Decoder Architecture", *IEEE Trans. on Communications*, vol. 56, no 12, pp. 1985-1989, Dec. 2008.
- [16] W. Oh and K. Cheun, "Joint decoding and carrier phase recovery algorithm for turbo codes," *IEEE Commun. Lett.*, vol. 5, no. 9, pp. 375-377, Sep. 2001.
- [17] C. Vanstraceele, J.P. Barbot, J.M. Brossier, B. Geller, "A Block Turbo Phase Synchronization Scheme", *IEEE Signal Processing Letters*, vol. 13 no 3, pp. 125-128, March 2006.
- [18] Colavolpe, A. Barbieri, and G. Caire, "Algorithms for iterative decoding in the presence of strong phase noise," *IEEE Journal on Selected Areas in Comm.*, Vol. 23, pp. 1748 - 1757, Sept. 2005.
- [19] V. Lottici and M. Luise, "Embedding carrier phase recovery into iterative decoding of turbo-coded linear modulations," *IEEE Trans. Commun.*, vol. 52, no. 4, pp. 661-669, Apr. 2004.
- [20] B. Geller, J.P. Barbot, J.M. Brossier, C. Vanstraceele, "System for Compensating Turbodecoder Phase Shift", US Patent App. 11/628,845.
- [21] C. Vanstraceele, B. Geller, J.P. Barbot, J.M. Brossier, "An Iterative Phase Synchronization Scheme for General QAM Constellations", *Proceedings of IEEE ICC*, Paris, June 2004.
- [22] L. Zhang and A. Burr, "Iterative carrier phase recovery suited for turbo-coded systems", *IEEE Trans. Wireless Commun.*, vol. 3, pp.2267-2276, Nov. 2004.
- [23] S. Bay, B. Geller, A. Renaux, J.P. Barbot, J.M. Brossier, "On the Hybrid Cramér-Rao bound and its Application to Dynamical Phase Estimation", *IEEE Signal Processing letters*, vol. 15, pp. 453-456, 2008.
- [24] J. Yang, B. Geller, and A. Wei, "Bayesian and Hybrid Cramer-Rao Bounds for QAM Dynamical Phase Estimation", *Proceedings of IEEE ICASSP'09*, Taipei, April 2009.
- [25] S. Bay, C. Herzet, J.M. Brossier, J.P. Barbot, B. Geller, "Analytic and Asymptotic Analysis of Bayesian Cramér-Rao Bound for Dynamical Phase Offset Estimation", *IEEE Transactions on Signal Processing*, vol. 56, no 1, pp. 61-70, Jan. 2008.
- [26] J. Yang, B. Geller, and A. Wei, "Approximate Expressions for Cramer-Rao Bounds of Coded Aided QAM Dynamical Phase Estimation", *Proceedings of IEEE ICC'09*, Dresden, June 2009.
- [27] J. Yang, B. Geller, and A. Wei, "Bayesian and Hybrid Cramer-Rao Bounds for QAM Dynamical Phase Estimation", *Proceedings of IEEE ICASSP'09*, Taipei, April 2009.
- [28] J. Dauwels and H.-A. Loeliger, "Phase Estimation by Message Passing", in *IEEE Intern. Conf. on Communications, ICC'04*, pages 523-527, Paris, France, June 2004.
- [29] M. Nissila and S. Pasupathy, "Adaptive Iterative Detectors for Phase-Uncertain Channels via Variational Bounding," *IEEE Trans. on Commun.*, vol. 57, pp.716-725, Mar. 2009.
- [30] H. Wymeersch, "Iterative Receiver Design", Cambridge Press.
- [31] J. Yang, B. Geller and S. Bay, "Bayesian and Hybrid Cramér-Rao Bounds for the Carrier Recovery under Dynamic Phase Uncertain Channels," *IEEE Trans. on Signal Processing*, vol. 59, no 2, Feb. 2011.
- [32] A. Cochran, Carrier Phase Synchronization by Reverse Playback. International patent PCT US 1997/022067, WO1998024210 on the 4th Jun. 1998.
- [33] J. Yang, B. Geller, C. Herzet, and J.M. Brossier, "Smoothing PLLs for QAM Dynamical Phase Estimation", *Proceedings of IEEE ICC'09*, Dresden, June 2009.
- [34] J. Yang, B. Geller and S. Bay, "Bayesian and Hybrid Cramer-Rao Bounds for the Carrier Recovery under Dynamic Phase Uncertain Channels," *IEEE Trans. on Signal Processing*, vol. 59, no 2, Feb. 2011.
- [35] L. Zhou, B. Geller, X. Wang, A. Wei, B. Zheng, H.C. Chieh, "Multi-user video streaming over multiple heterogeneous wireless networks: a distributed, cross-layer design paradigm", *Journal of Internet*, vol. 10, no 1, 2009.
- [36] I. Akyildiz, M. Can Vuran "Wireless Sensor Networks", Wiley, 2010.